Time-dependent perturbation of Mössbauer spectra

Markku Salkola* and Stig Stenholm
Research Institute for Theoretical Physics, University of Helsinki, Siltavuorenpenger 20C, SF-00170 Helsinki, Finland
(Received 8 June 1989)

In this paper we derive a complete semiclassical description of Mössbauer spectroscopy with arbitrary external or internal perturbations of the active levels. The γ rays are taken to be weak enough to allow us to evaluate the linear Mössbauer response to lowest order in the intensity, in which case the γ-ray field can be treated classically. It induces transitions between level manifolds that can have arbitrary interactions inside themselves. The nuclear system is described by a density matrix. In principle, time-dependent perturbations can be handled by the formalism, but the equations are easier to solve for systems that display steady-state behavior. We consider, in particular, the case of magnetic radio-frequency modulation of the Mössbauer levels. Utilizing a matrix-continued-fraction technique, we solve for the absorption spectrum, and we choose numerical illustrations with parameters such that they describe the nucleus ^{57}Fe. In this paper we treat mainly the case of magnetic modulation, but other experimental arrangements are discussed too. The calculations are able to treat both saturation and interference effects, which become important when the radio-frequency modulation is very strong. The new feature that emerges is the occurrence of resonances arising from the interference of different physical processes. The calculational method and its results are discussed and compared with other works.

I. INTRODUCTION

In an early work,[1] Perlow investigated how a magnetic modulation affects Mössbauer spectra, and discussed the physical mechanisms involved. An oscillating magnetic field is found to distort the spectral lines or split them into subcomponents, see Refs. 2–7. Similar phenomena involving optical photons have been discussed in Ref. 8. The observed behavior may derive from several physical effects; in addition to Zeeman modulation of the energy levels, the spectral parameters may be affected by the motion of magnetic domain walls or mechanical distortion caused by magnetostriction.

For a magnetically soft material, a weak external magnetic field may become amplified at the position of the nucleus. If the rf modulation effect can be described by a simple periodic variation of the level spacing, a moderate modulation frequency can be seen as sidebands on the main resonance, but when the frequency of modulation is increased, the spectrum first becomes distorted and finally coalesces into its main components. This corresponds to the motional narrowing limit of random-field-induced relaxation. The occurrence of pure Zeeman modulation was suggested by Ref. 9, and recently experimental confirmation has been obtained in the work.[10] The transients due to magnetic Zeeman modulation were described by a purely classical phase-modulation theory in Ref. 10.

In this work we develop a theory for Mössbauer spectroscopy under the influence of a rf magnetic field. The approach is based on a semiclassical picture where all fields are treated as classical entities, but the nuclear level scheme is described by quantum mechanics. The spontaneous emission of γ quanta in the presence of a radio-frequency field was calculated in Ref. 11. We are treating an absorber, but in the limit of low γ intensity, the emitter can be discussed in exactly the same manner. For phenomena that occur to second order in the coupling to the radiation field no quantum effects are expected. The ensuing density-matrix equations are solved as matrix-continued fractions allowing arbitrary field configurations and polarizations. Our examples involve only magnetic interactions, but the level scheme used can easily be generalized to include, e.g., electric quadrupole interactions. This case is interesting because it removes the spin degeneracy only partially, and we plan to discuss it in a separate publication.

A common feature of all previous Mössbauer calculations treating a transverse rf magnetic field is that they consider a pure rotating field or approximate their configuration by such a field, see, e.g., Refs. 11–13. This so-called rotating-wave approximation does not allow the exchange of rf photons of different polarization in the same interaction process. Our results will, consequently, differ from those of the earlier works, especially for large rf amplitudes; see the examples calculated in Sec. IV. In addition most works introduce some further simplification in their calculated models. The observations are, however, performed with linearly polarized transverse fields, and the rotating-wave approximation is not applicable. In the experiments, the nucleus can exchange rf photons of both polarizations alternatively; this gives rise to interference effects which have not been included in the calculations previously. Such complicated situations can be treated in a straightforward way by the matrix-continued-fraction method without the introduc-

tion of any approximations.

Because the γ-ray intensity is always small, it is taken into account only in the lowest approximation; we evaluate the linear Mössbauer response under the influence of perturbing fields. These other interactions, internal or external, are retained exactly. Thus we obtain a new theoretical description of steady-state spectroscopy which allows the evaluation of the effects of various physical agents acting on Mössbauer systems. The formalism could be utilized directly to calculate the effects of a stochastic perturbation. Here we, however, apply it to the modulation effects caused by a radio-frequency magnetic field imposed externally. The steady-state results can be obtained exactly, and saturation and interference effects can be calculated. For a large enough modulation, the latter are found to give rise to new resonances, but these require amplitudes that are, probably, experimentally unrealistic.

The solution utilizes continued fraction methods in an essential way. Earlier these have been applied successfully to a broad class of resonance phenomena. Using ordinary continued fractions Autler and Townes[14] analyzed the ac Stark effect, and Stenholm and Lamb[15] solved the optical Bloch equations of a two-level atom in a standing wave. Stenholm[16,17] introduced the same method in the context of rf multiphoton resonances for incoherent pumping of the Zeeman levels. Allegrini, Arimondo, and Bambini[18] used a matrix-continued fraction to solve a two-level problem, and Valli and Stenholm[19] generalized the treatment to multilevel systems. The method is discussed in detail in the monograph by Risken.[20]

The outline of the paper is as follows. All necessary definitions and the formulation of the problem are found in Sec. II. Since all fields are either periodic or constant, we are able to write the semiclassical equation of motion as a vector recurrence relation, which can be solved by matrix-continued fractions. This is carried out in Sec. III. In Sec. IV we demonstrate the method by a few examples of evaluated spectra. Finally, Sec. V contains some concluding remarks.

II. FORMULATION OF THE CALCULATION

We are going to discuss Mössbauer transitions between two manifolds of levels shown in Fig. 1. The transition $1\leftrightarrow 2$ is induced by γ quanta of energy $\hbar\omega_0$. Within each manifold the energy is degenerate due to the nuclear spin I_i $(i=1,2)$. When the degeneracy is removed, the levels split into sublevels spaced by radio-frequency energy differences. The main source of the splitting is the magnetic field B acting at the site of the nucleus. If the nuclear g factor is denoted by g_i the energy splitting becomes

$$E_i=-g_i\mu_N m_I B \ , \tag{1}$$

where the magnetic quantum number is $m_I\in\{-I_i,\ldots,I_i\}$; μ_N is the nuclear magneton. In the following we will usually take metallic ^{57}Fe as our example, and here the magnetic field comes mainly from the internal hyperfine field which is about $33T$.

If the nucleus has a quadrupole moment Q, it adds to the splitting. This is a tensor quantity, but for simplicity we assume that we can take its component along the same quantization z axis as in Eq. (1). Then the splitting is

$$E_Q=\frac{eQV_{zz}}{2I(2I-1)}[3m_I^2-I(I+1)] \ . \tag{2}$$

Here V_{zz} is the electric field gradient in the z direction. The quantities I and Q take different values in the levels 1 and 2. For substances without an internal field the main splitting is due to the quadrupole, which is insensitive to the sign of the magnetic quantum number m_I. The quadrupole will make the magnetic splitting (1) asymmetric.

The coupling between the upper and lower levels of the two manifolds is affected by an operator of the form

$$H_{12}=\sum_{m_1,m_2,k} G_k(m_1,m_2)(|1,m_1\rangle\langle 2,m_2|a_k + |2,m_2\rangle\langle 1,m_1|a_k^\dagger) \ , \tag{3}$$

where $a_k^\dagger$ creates a γ photon in the state labeled by k, and G is the appropriate coupling constant. In (3) we have only retained the energy conserving transitions, which is called the rotating-wave approximation in spin-resonance physics. We are going to use the coupling (3) to second order, which implies that we will encounter only single-particle averages of the boson operators like $\langle a^\dagger a\rangle$, and from optical phyisics it is well known that these first-order correlation functions can be calculated from a semiclassical approximation. In the following we thus replace the boson operators by classical fields oscillating at a frequency ω in the γ energy range. For our purposes it also suffices to look at one frequency at a time; this can be thought of as the frequency of the detector. The dependence on ω is equivalent with the recorded Mössbauer spectra.

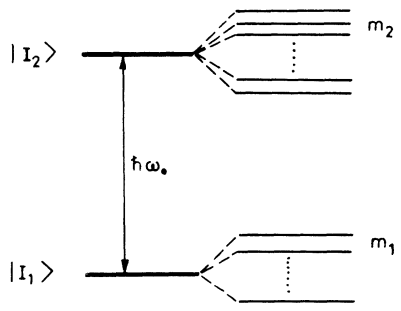

FIG. 1. The two Mössbauer levels with spin I_i $(i=1,2)$ have an average energy spacing $\hbar\omega_0$, which is supposed to be in the γ-ray range. Each level is degenerate and its sublevels can be split apart by internal or externally imposed perturbations.

We utilize a block matrix representation. When the upper level has the degeneracy

$$M=2I_2+1 \tag{4}$$

and the lower level the degeneracy

$$N=2I_1+1\ , \tag{5}$$

the representation becomes

$$H=\begin{bmatrix}(M\times M) & (M\times N)\\ (N\times M) & (N\times N)\end{bmatrix}\ . \tag{6}$$

In this representation the Hamiltonian we are going to discuss follows from Eqs. (1) to (3) in the form

$$H=\frac{\hbar\omega_0}{2}\begin{bmatrix}1 & 0\\ 0 & -1\end{bmatrix}-\begin{bmatrix}g_2\mu_N\hat{I}_2B & 0\\ 0 & g_1\mu_N\hat{I}_1B\end{bmatrix}+\begin{bmatrix}E_Q^{(2)} & 0\\ 0 & E_Q^{(1)}\end{bmatrix}+\hbar E\begin{bmatrix}0 & D^{(+)}\\ D^{(-)} & 0\end{bmatrix}\ . \tag{7}$$

The coupling $D^{(\pm)}$ is to be obtained from the multipole coupling between the γ levels induced by the effective semiclassical γ-ray field

$$E=E_0\cos\omega t \tag{8}$$

and the quantity $|D|^2=D^{(+)}D^{(-)}$ is proportional to the coupling between the nuclear levels including the proper Clebsch-Gordan coefficients between the spins $I_1\leftrightarrow I_2$. The matrix elements depend on the multipole nature of the transition; for ^{57}Fe the transition is of the magnetic dipole type $M1$. The same elements appear in the multipole expectation value induced by the γ radiation.

We use a block representation of the density matrix corresponding to the form (6) including the γ frequency explicitly

$$\rho=\begin{bmatrix}\rho_{22} & e^{-i\omega t}\tilde{\rho}_{21}\\ e^{i\omega t}\tilde{\rho}_{12} & \rho_{11}\end{bmatrix}\ . \tag{9}$$

Using Eqs. (8) and (9) we can write the absorbed energy in the form

$$\mathcal{A}=\left\langle E\frac{dP}{dt}\right\rangle_{\rm av}=\left\langle E\frac{d}{dt}\mathrm{Tr}\left[\rho\begin{bmatrix}0 & D^{(+)}\\ D^{(-)} & 0\end{bmatrix}\right]\right\rangle_{\rm av}=C\ \mathrm{Im}[\mathrm{Tr}(D^{(+)}\tilde{\rho}_{12})]\ . \tag{10}$$

Here $\langle\ \rangle_{\rm av}$ denotes a time average, and a constant of proportionality C has been introduced for convenience.

The equation of motion for the density matrix is, as usual,

$$i\hbar\frac{\partial\rho}{\partial t}=[H,\rho]+\mathcal{R}(\rho)\ , \tag{11}$$

where the operator $\mathcal{R}$ symbolizes all relaxation terms needed. The Hamiltonian (7) is written in the block form

$$H=\hbar\begin{bmatrix}h_2 & D^{(+)}\\ D^{(-)} & h_1\end{bmatrix}\ . \tag{12}$$

The equation for the off-diagonal block now becomes

$$\left(i\frac{\partial}{\partial t}-\omega\right)\tilde{\rho}_{12}=h_1\tilde{\rho}_{12}-\tilde{\rho}_{12}h_2+D^{(-)}\rho_{22}-\rho_{11}D^{(-)}+\mathcal{R}(\tilde{\rho}_{12})\ . \tag{13}$$

Because we need to solve the equation only to lowest order in the γ-ray coupling constant, we can insert the diagonal blocks in their unperturbed forms into Eq. (13). As we treat the absorber case we can set ρ_{22} equal to zero and replace ρ_{11} by a constant quantity $\rho_{11}^{(0)}$, which is the steady-state distribution function for the lower level in the sample.

Equation (13) is a linear equation in ρ which can be solved formally by a linear operator $\mathcal{U}$ in the form

$$\tilde{\rho}_{12}=\mathcal{U}(\rho_{11}^{(0)}D^{(-)})\ . \tag{14}$$

For a time-independent problem the Fourier transform may be used to obtain $\mathcal{U}$, for time-dependent cases other techniques have to be developed. When (14) is inserted into Eq. (10) we obtain the expression

$$\begin{aligned}\mathcal{A}&=C\ \mathrm{Im}\{\mathrm{Tr}[\mathcal{U}(\rho_{11}^{(0)}D^{(-)})D^{(+)}]\}\\ &=C\ \mathrm{Im}\{\mathrm{Tr}[\rho_{11}^{(0)}D^{(-)}\mathcal{U}^\dagger(D^{(+)})]\}\\ &=C\ \mathrm{Im}\langle D^{(-)}\mathcal{U}^\dagger D^{(+)}\rangle_0\ .\end{aligned} \tag{15}$$

Here we have introduced the operator $\mathcal{U}^\dagger$ which is the adjoint of $\mathcal{U}$ with respect to the trace as a scalar product. Because the density-matrix time evolution is not unitary this operator is not the inverse of $\mathcal{U}$. The subscript zero indicates that the average is taken over the equilibrium distribution function in the lower state manifold. The form (15) is similar to an expression derived by Fano[21] and agrees with the conventional view that the observed spectrum is the Fourier transform of the correlation function

$$K(t)=\langle D^{(-)}D^{(+)}(t)\rangle\ , \tag{16}$$

where the operators are in the Heisenberg representation.

To show the consistency of our view we evaluate the expression (15) for the case of no interactions in the manifolds 1 and 2. In this case the states can be labeled by the magnetic quantum numbers m_1 and m_2, and we obtain from Eq. (13)

$$\langle m_1|\rho_{12}|m_2\rangle=-\frac{E}{2}\frac{\langle m_1|D^{(-)}|m_2\rangle}{\omega-\Delta E(m_2,m_1)+i\Gamma}\rho_{11}^{(0)}(m_1)\ , \tag{17}$$

which inserted into Eq. (15) gives the expression

$$\mathcal{A}=C'\sum_{m_1,m_2}|\langle m_1|D^{(-)}|m_2\rangle|^2\frac{\Gamma}{[\omega-\Delta E(m_1,m_2)]^2+\Gamma^2}\ , \tag{18}$$

which agrees with the conventional expression for Mössbauer spectra. We have assumed one relaxation rate

only; this can easily be generalized. The energy difference is

$$\Delta E(m_2,m_1)=\omega_0-\mu_N(g_2m_2-g_1m_1)B+E_Q^{(2)}-E_Q^{(1)}\ , \tag{19}$$

where both the magnetic dipole energy (1) and the quadrupole energy (2) have been written out. The coefficient $|D|^2$ contains the Clebsch-Gordan coefficients appropriate for the γ transition being investigated.

In this section we have reformulated the Mössbauer measurement in a manner which is useful for our purposes in the following. In Sec. III we are going to see how to apply this formalism to the case of periodic modulation of the magnetic sublevels.

III. PERIODIC MODULATION

The formulation of the Mössbauer measurement given above is, in principle, applicable also to the case of time-dependent Hamiltonians. However, in this case the operator $\mathcal{U}$ of Eq. (14) becomes much harder to obtain. For a random noise modulation, the techniques of stochastic processes can be used. This was done in a slightly different formalism by Dekker[22] and Blume and coworkers.[23] In our formulation we could apply the methods developed in laser physics[24] to recover these results. For a strictly periodic modulation the continued-fraction techniques[18–20] are useful.

Here we assume only one single frequency Ω in the external modulation and use the radio-frequency magnetic field

$$B(t)=B\cos\Omega t\ . \tag{20}$$

The observed quantities are assumed to be time averages over a large number of radio-frequency periods. This is also equivalent with an ensemble average taken after a time long enough to damp out initial transients.

There are two dimensionless parameters in the theory. If we introduce a Larmor frequency

$$\Omega_0=g\mu_N B/\hbar \tag{21}$$

characteristic of the spin resonances, which are all of the same order of magnitude, we have the quantities

$$\xi=\frac{\Omega}{\Gamma},\quad \eta=\frac{\Omega_0}{\Omega}\ . \tag{22}$$

When η is small we are in the weak modulation limit and the response to the modulation can be obtained in perturbation theory. Because the width of the nuclear levels is Γ, a small value of ξ indicates that the modulation gives an oscillation within the linewidth only; this is the slow modulation case. For a large ξ the frequency of the resonances is displaced by more than the linewidth; this is the fast modulation limit.

To see an explicit example of our approach and the physical features of the result, we look at the simple case shown in Fig. 2. We have a two-level system, the frequency separation of which is varied periodically at the frequency Ω. We calculate the response of this as an absorber using the formalism developed above. The Hamiltonian is taken in the form

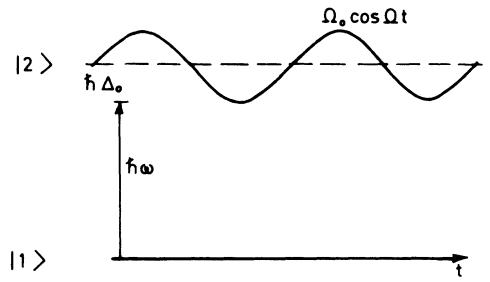

FIG. 2. Our model consist of two levels with a periodically varying spacing; for simplicity we ascribe this to the upper level only. The probing frequency ω is detuned by the amount Δ_0 from the average transition frequency. When this is tuned through resonance, the response traces out the shape of the observed spectrum.

$$H=\begin{bmatrix}\Delta_0+\Omega_0\cos\Omega t & d\\ d^* & 0\end{bmatrix}\ , \tag{23}$$

where the detuning

$$\Delta_0=\omega_0-\omega \tag{24}$$

gives the photon's energy deficiency in affecting the γ transition. The parameter ω_0 is the central γ frequency; by tuning the detected frequency ω across this we record the shape of the observed spectrum. The Hamiltonian (23) is seen to be of the type (12). In perturbation theory we assume all population on the lower level and set

$$\rho_{11}\approx 1,\quad \rho_{22}\approx 0\ . \tag{25}$$

The off-diagonal density matrix element satisfies then the equation of motion

$$i\frac{\partial}{\partial t}\tilde{\rho}_{21}=(\Delta_0+\Omega_0\cos\Omega t-i\Gamma)\tilde{\rho}_{21}+d\ . \tag{26}$$

This equation can be solved in steady state by the use of the Fourier decomposition

$$\rho_{21}=\sum_{k=-\infty}^{+\infty} r_k e^{ik\Omega t}\ , \tag{27}$$

which gives the recurrence relation

$$(k\Omega+\Delta_0-i\Gamma)r_k+\tfrac{1}{2}\Omega_0(r_{k+1}+r_{k-1})=-d\delta_{k,0}\ . \tag{28}$$

It is straightforward to solve this in the form of a continued fraction (see, e.g., Ref. 16) to obtain the result of the absorption (10)

$$\mathcal{A}=\mathrm{Im}d^*r_0\ . \tag{29}$$

The present problem is, however, simple enough to allow an analytic solution. Using the properties of the Bessel functions $J_n(x)$, we easily see that the expression

$$r_k=-d\sum_{l=-\infty}^{+\infty}J_l\left[\frac{\Omega_0}{\Omega}\right]J_{l-k}\left[\frac{\Omega_0}{\Omega}\right]\frac{1}{\Delta_0+l\Omega-i\Gamma} \tag{30}$$

solves the recurrence relation (28). The observed spectrum (29) is now given by

$$\mathcal{A}=\frac{|d|^2}{\Gamma}\sum_{k=-\infty}^{+\infty}J_k^2(\eta)\frac{1}{[(\Delta_0/\Gamma)-k\xi]^2+1} . \tag{31}$$

This is the well-known result for frequency-modulated subbands. The physical features are seen very clearly from this expression. For a weak modulation $\eta\ll 1$ the Bessel functions disappear rapidly and only the central peak $k=0$ survives. The corrections come from the terms $k=\pm 1$. For a small value of ξ many sidebands fall within one linewidth and the line seems to be broadened. When ξ becomes large the sideband resonances become well resolved assuming that the Larmor frequency Ω_0 is large enough to give sufficient sideband intensities. Physically this means that the modulation of the two-level transition $1\leftrightarrow 2$ must be faster than the rate of change of this modulation. Only in this case can the information about the modulation frequency Ω be transmitted to the observed spectrum. If this modulation frequency grows, the spectrum (31) reduces to the central line in all cases. Because of the Bessel function sum rule

$$\sum_{k=-\infty}^{+\infty}J_k^2=1 , \tag{32}$$

the total intensity of the spectrum integrated over the γ frequency ω remains constant. This sharpening of the spectrum towards the central line is a manifestation of the motional narrowing phenomenon.

We generalize the present treatment by looking at the Hamiltonian (12) with a periodically modulated part

$$H=\hbar\begin{bmatrix}h_2 & D^{(+)}\\ D^{(-)} & h_1\end{bmatrix}+\hbar\begin{bmatrix}V_2 & 0\\ 0 & V_1\end{bmatrix}\cos\Omega t . \tag{33}$$

For simplicity we neglect the quadrupole contribution (2) to the spectrum and write

$$V_i=\alpha_i\hat{I}_{ix}+\beta_i\hat{I}_{iz} . \tag{34}$$

Here we have assumed that the modulation is achieved with a radio-frequency magnetic field that can have both a transverse ($\perp$) and a longitudinal ($\parallel$) component. The parameters in (34) are

$$\begin{aligned}\alpha_i&=-g_i\mu_N B_{\perp}^{\mathrm{rf}}/\hbar ,\\ \beta_i&=-g_i\mu_N B_{\parallel}^{\mathrm{rf}}/\hbar,\quad (i=1,2) .\end{aligned} \tag{35}$$

With the density matrix in the form of Eq. (9) we obtain the equation of motion

$$\left[i\frac{\partial}{\partial t}-\omega\right]\tilde{\rho}_{12}=(h_1+V_1\cos\Omega t)\tilde{\rho}_{12}-\tilde{\rho}_{12}(h_2+V_2\cos\Omega t)-\rho_{11}^{(0)}D^{(-)}-\frac{i}{2}\Gamma_{11}\tilde{\rho}_{12}-\frac{i}{2}\tilde{\rho}_{12}\Gamma_{22} . \tag{36}$$

Here we have retained the possibility that the relaxation matrices Γ_i can be different inside the manifolds 1 and 2.

To obtain the steady-state solution for (36) we replace the $(N\times M)$-dimensional density matrix by a one-dimensional array and expand this in the Fourier series

$$\tilde{\rho}_{12}=\sum_{k=-\infty}^{+\infty}R(k)e^{ik\Omega t} . \tag{37}$$

The matrices in (36) now become $[(N\times M)\times(N\times M)]$-dimensional matrix operators (sometimes called superoperators), which we denote by underlines. After the insertion of (37) Eq. (36) now becomes

$$(k\Omega+\underline{H}-i\Gamma)R(k)+\tfrac{1}{2}\underline{V}[R(k+1)+R(k-1)]=-\underline{D}\rho_{11}^{(0)}\delta_{k,0} . \tag{38}$$

Here we have introduced the quantity $\underline{D}\rho_{11}^{(0)}$ as an $N\times M$ vector representing the equilibrium density matrix of the lower level 1. This recurrence relation can be solved using matrix-continued-fraction techniques as applied to these types of problems in Refs. 18–20.

Because of the imaginary part $i\Gamma$, the operator in the first term of (38) can be inverted and we can write the equation in the form

$$R(k)+\underline{A}(k)[R(k+1)+R(k-1)]=-\underline{L}(0)\underline{D}\rho_{11}^{(0)}\delta_{k,0} . \tag{39}$$

Here we have defined

$$\begin{aligned}\underline{A}(k)&=\tfrac{1}{2}\underline{L}(k)\underline{V} ,\\ \underline{L}(k)&=\frac{1}{k\Omega+\underline{H}-i\Gamma} .\end{aligned} \tag{40}$$

To solve (39) we define the operators $\underline{L}^{\pm}$ by setting

$$\begin{aligned}R(k)&=\underline{L}^{+}(k)R(k-1)\quad (k>0)\\ R(k)&=\underline{L}^{-}(k)R(k+1)\quad (k<0) .\end{aligned} \tag{41}$$

The time-averaged observable requires the component $R(0)$, which we can solve as

$$\begin{aligned}R(0)&=-\frac{1}{1-\underline{A}(0)[\underline{L}^{+}(1)+\underline{L}^{-}(-1)]}\underline{L}(0)\underline{D}\rho_{11}^{(0)}\\ &\equiv\underline{U}\underline{D}\rho_{11}^{(0)} ,\end{aligned} \tag{42}$$

which defines the operator $\underline{U}$ analogously with the operator $\mathcal{U}$ in Eq. (14).

From Eq. (39) we obtain the recurrence relations for the operators $\underline{L}^{\pm}$

$$\underline{L}^{\pm}(k)=-\frac{1}{1+\underline{A}(k)\underline{L}^{\pm}(k\pm 1)}\underline{A}(k) . \tag{43}$$

These equations are easily evaluated iteratively on the computer. To avoid convergence difficulties caused by round-off errors, the iteration starts from a large value of k, and all vector components outside this are set equal to zero. Then the iteration proceeds towards the values $k=\pm 1$ which gives $R(0)$ from Eq. (42).

Once the vector $R(0)$ has been obtained the observable quantity (10) becomes

$$\mathcal{A}=\mathrm{Im}[\mathrm{Tr}(D^{(+)}\tilde{\rho}_{12})]=\mathrm{Im}\langle \underline{D}^{\dagger},\underline{UD}\rho_{11}^{(0)}\rangle \ . \tag{44}$$

The scalar product $\langle\ \rangle$ is defined in the $N\times M$-dimensional vector space of the matrix ρ_{12}. With these tools we can solve the problem of radio-frequency modulation of the Mössbauer spectrum completely in terms of matrix-continued fractions. In Sec. IV we look at some special cases of physical interest.

IV. CALCULATED EXAMPLES

We next fix our numerical parameters to correspond approximately to the specific case of the 14-keV Mössbauer resonance in ^{57}Fe. This is an $M1$ transition of the type $\frac{3}{2}^{(-)}\leftrightarrow\frac{1}{2}^{(-)}$, where the magnetic dipole transition conserves the parity $(-)$. The level structure is shown in Fig. 3. The internal magnetic field splits the levels by Δ_1 and Δ_2 in the lower and upper levels, respectively. With sufficient accuracy we can take the nuclear g factors to be $g_2\simeq -0.1$ and $g_1\simeq 0.2$; this implies that the levels are inverted with respect to the ordering of the magnetic quantum numbers in the two levels. The result is the well-known six-line spectrum, where the dipole transitions, with $|\Delta m|\le 1$, have their strengths determined from the Clebsch-Gordan coefficients by the equation

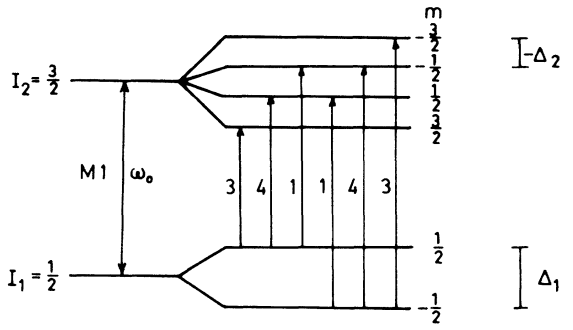

FIG. 3. This shows the level scheme of the 14.4-keV Mössbauer transition in ^{57}Fe. The splittings in the two levels are in opposite directions, which leads to the characteristic six-line spectrum. The parameters in the text are chosen to approximately describe this case.

$$\langle I_2m_2|D^{(+)}|I_1m_1\rangle\langle I_1m_1'|D^{(-)}|I_2m_2'\rangle\propto\sum_{M,M'}D_{Mq}^{(L)}(\varphi,\theta,0)[D_{M'q}^{(L)}(\varphi,\theta,0)]^{*}\langle I_1Lm_1M|I_2m_2\rangle\langle I_1Lm_1'M'|I_2m_2'\rangle \ . \tag{45}$$

Here $D_{Mq}^{(L)}(\alpha,\beta,\gamma)$ is the rotation matrix element for the Euler angles α,β,γ. In the present case the observed Mössbauer spectrum is not averaged over the direction of the magnetic field, and we choose the angles $\varphi=\theta=\pi/2$. For ^{57}Fe this gives the ratios 3:4:1:1:4:3 for the line intensities. In thermal equilibrium the population on the lower level is given by the canonical distribution

$$\rho_{11}^{(0)}=\frac{\exp(-\hbar h_1/k_BT)}{\mathrm{Tr}[\exp(-\hbar h_1/k_BT)]} \ . \tag{46}$$

In ^{57}Fe the energy differences are given mainly by the splitting due to the internal magnetic field of about 33 T. This, however, corresponds to a temperature of only about 2 mK, and consequently the experiment is usually performed at a high temperature giving an even distribution over the internal states

$$\rho_{11}^{(0)}(m_1)=\frac{1}{N} \ , \tag{47}$$

where N is the lower state degeneracy in Eq. (5). In the observed quantity (44), the choice (47) will give a constant prefactor only; this can be omitted in the following.

When we map the density matrix elements of ρ_{12} into an array R as in Eq. (38), the enumeration of the components of R can be chosen as the following:

$$(\rho_{12})_{ij}\equiv R_{M(j-1)+i}\quad (i\in\{1,M\};j\in\{1,N\}) \ . \tag{48}$$

This way there is a unique one-to-one mapping between the elements. With this representation of the density matrix the observable result in Eq. (44) can be written

$$\mathcal{A}=\mathrm{Im}\sum_{\substack{k,l\\k',k'}}\underline{D}^{*}_{M(l-1)+k}\underline{U}_{M(l-1)+k;M(l'-1)+k'}\underline{D}_{M(l'-1)+k'} \ . \tag{49}$$

This is the equation used to evaluate the observed spectra numerically.

We take the following parameters for the splittings:

$$\Delta_2/\Gamma=-25,\quad \Delta_1/\Gamma=50 \ , \tag{50}$$

where we have chosen the resonance linewidth $(\Gamma/2\pi)\approx 10^6\ \mathrm{s}^{-1}$ as the unit. In a given radio frequency field configuration the ratio of the g factors gives the ratios

$$\alpha_1/\alpha_2=\beta_1/\beta_2=-2 \ , \tag{51}$$

where α and β are given by Eq. (35). In order to illustrate the method and verify that the results are intuitively acceptable, we choose the simple case $\alpha_i=0$ first. This gives a purely longitudinal rf field, which only modulates the frequency of each sublevel without mixing the levels. In Fig. 4 we show the spectra, when the radio frequency is fixed at $\Omega=10\Gamma$ and the longitudinal magnetic field is increased. We label the graphs with the upper-level splitting $\beta_2\in(0,10)$, but from Eq. (34) we can see that each level experiences a different modulation amplitude de-

pending on its magnetic quantum numbers. Because the g factor in the lower level is twice that in the upper we find the modulation ratios 5:3:1:1:3:5. In Fig. 4 we can see how each line independently shows a Bessel function sideband structure according to the result (31). The splittings increase and more sidebands appear for an increased modulation; the effect is strongest at the outermost lines because these correspond to the largest quantum numbers.

Next we look at the purely transverse case. Then we have $\beta_i = 0$, and the radio-frequency transitions can mix the sublevels inside the manifolds. In Fig. 5 we have fixed the modulation coefficients at $\alpha_1 = -2\alpha_2 = 10\Gamma$, and the radio frequency Ω is increased from the small value 20Γ to infinity. The latter case corresponds to no modulation, as we explained in connection with Eq. (31). In the figure we can see how an increased modulation frequency complicates the pattern, but for the two values $\Omega = 50\Gamma$ and 25Γ the pattern is clear and admits an easy physical explanation. In the former case the radio frequency achieves resonance with transitions in the lower manifold and the lines show a dynamic Stark splitting into doublets. In the latter case resonance occurs in the upper manifold and the lines are split into four components. For an infinite modulation frequency the unperturbed spectrum is found. For the intensity used in Fig. 5 the rotating-wave approximation holds good, and our treatment is essentially equivalent with those obtained by

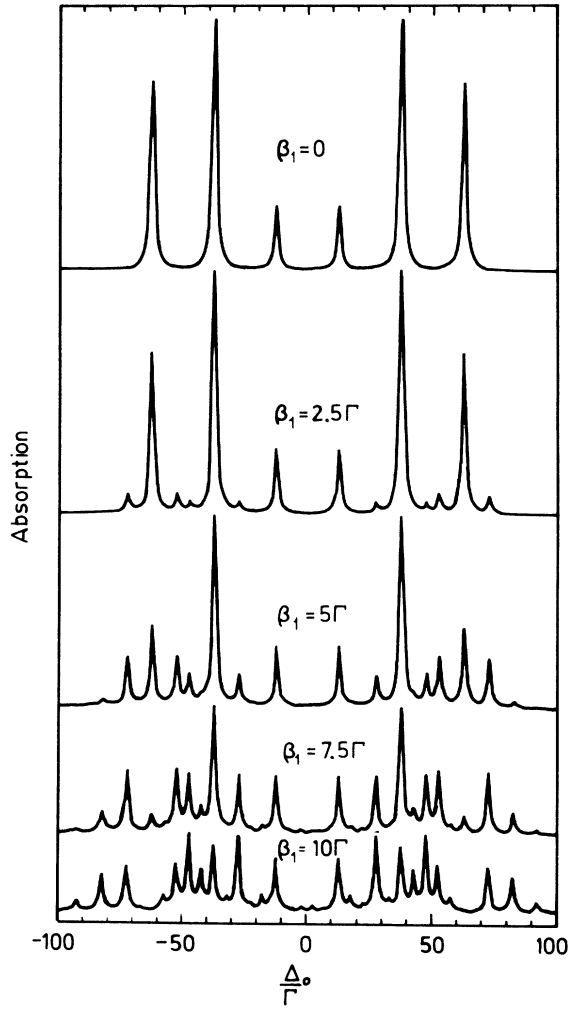

FIG. 4. This shows the absorption spectrum as a function of detuning from the average transition frequency, when the longitudinal field amplitude β is increased. The case is simple, and each line acquires its own sidebands with strengths determined by the Bessel functions [cf. Eq. (31)]. The other parameters are $\Delta_2 = -25\Gamma$, $\Delta_1 = 50\Gamma$, and $\Omega = 10\Gamma$, which leads to well-resolved resonances.

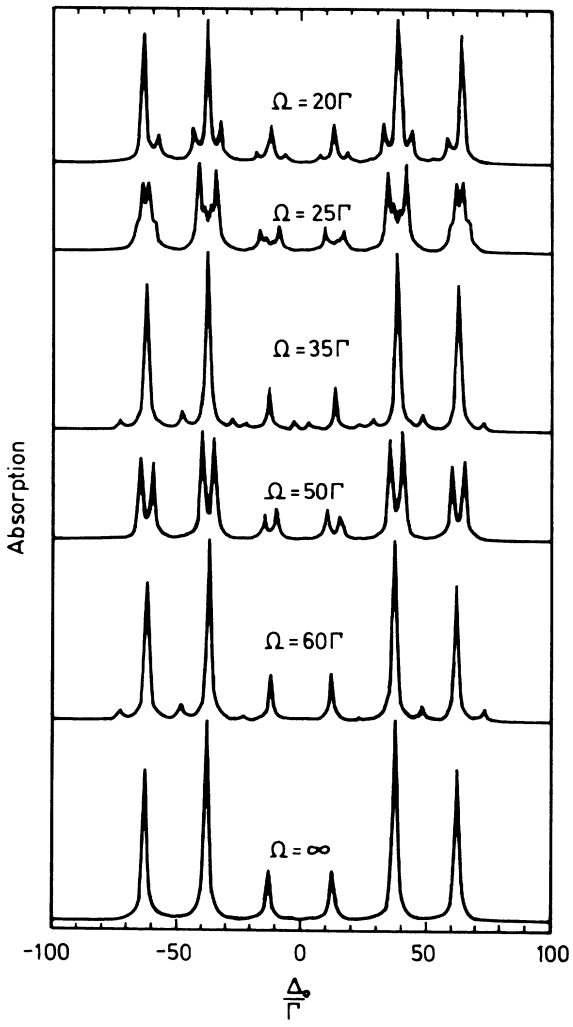

FIG. 5. This shows spectra like those in Fig. 4, but for a purely transverse field. The intensity is chosen to be such that $\alpha_1 = 10\Gamma$, and the rf frequency is increased. The other parameters are as in Fig. 4. For the two values $\Omega = 25\Gamma$ and 50Γ, the sidebands couple the levels resonantly in the upper and lower submanifolds, respectively. Each line is then split according to the multiplicity of the manifold by the dynamic Stark shift.

Hack and Hammermesh[11] and Gabriel.[12]

For larger modulation amplitudes the various effects are less easily seen. In Fig. 6 we show a spectrum like that in Fig. 5 but with the increase modulation intensity $\alpha_1 = -2\alpha_2 = 50\Gamma$. The same trends as seen in Fig. 5 can be discerned in Fig. 6. It shows, however, a distortion of the line shape and additional resonances between the main ones. These are the multiphoton resonances known from radio-frequency spectroscopy.[14-17] In this case they show up for large modulation amplitudes only; the values of α correspond to a magnetic modulation amplitude of up to $15T$. Thus it may not be realistic to attempt to observe them experimentally at the present state of the art.

We have also applied the formalism to the case of a pure quadrupole splitting according to Eq. (2). In this case the sublevels with $\pm m$ remain degenerate, and the transition $\frac{3}{2} \leftrightarrow \frac{1}{2}$ becomes a doublet with the energy splitting given by

$$\Delta = \tfrac{1}{2} eQV_{zz} \ . \tag{52}$$

When, e.g., a transverse modulation mixes the levels, each component of the doublet is, at resonance $\Omega = \Delta$, split into a pair of levels corresponding to the dynamic Stark splitting of the upper manifold levels, which have become coupled by the radio-frequency field. The details of the treatment can be worked out in a straightforward way.

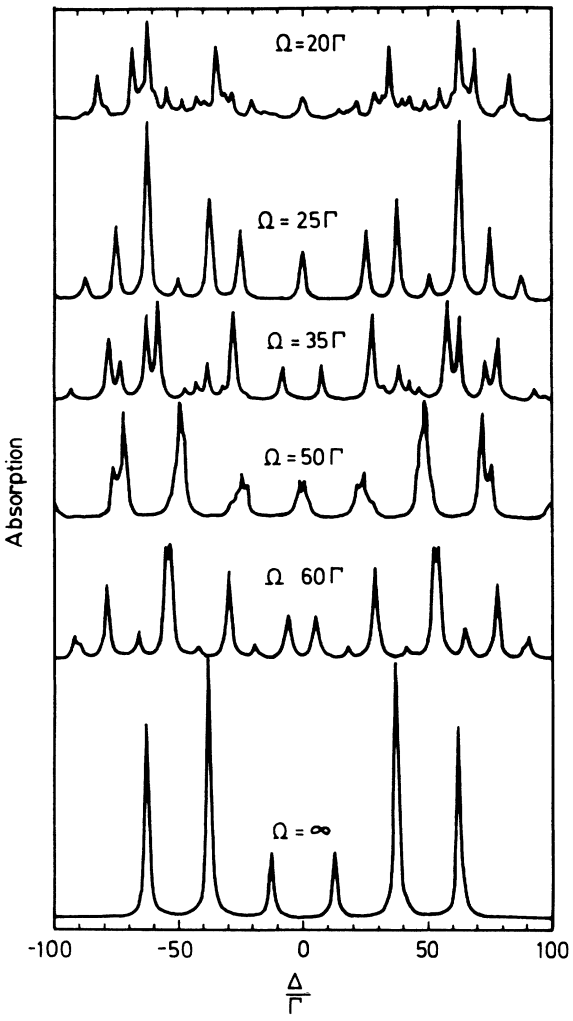

FIG. 6. This figure shows the same spectra as Fig. 5 but for the stronger rf field $\alpha_1 = 50\Gamma$; all other parameters are the same. A comparison shows that the spectra have become more complex; in some parameter ranges additional resonances are seen. These features derive from interferences between various physical processes that acquire additional importance when the field amplitude is increased.

V. GENERALIZATIONS AND CONCLUSIONS

The calculations above contain several assumptions. Some of these are harmless because they are essential to the physical situation characterizing Mössbauer spectroscopy. In common with optical spectroscopy is the fact that the frequency of the radiation is the largest frequency parameter of the problem by a large factor. Hence all contributions proportional to any power of ω^{-1} can be neglected; in particular the rotating-wave approximation for the γ radiation is excellent. The linewidth is narrow and the various radiative transitions are well separated. It is thus possible to separate a single pair of level manifolds and consider γ transitions between them without interference from other γ active levels. Finally there are only a few γ quanta present at any one time. Thus the gamma intensity is always low, and no saturation effects need be considered. The radiation is also incoherent, and no definite phase relationship between the γ radiation and the radio-frequency field must be introduced. In the present semiclassical calculation the observable results must be independent of the phase of the radiation.

Some other assumptions are inessential; they are introduced only to simplify the calculations. We have assumed a simple periodic time dependence of the type (20). This leads to the simple recurrence relation (38), which allows the continued-fraction solution. The method in itself is valid for a more general time evolution. It only becomes a more complicated problem to evaluate the operator $\mathcal{U}$ of Eq. (14). The other simplifying assumption is the high-temperature form (47) of the lower-level distribution function. The result is trivially generalized to the thermal distribution (46). It is also possible to calculate the lower-level distribution function $\rho_{11}^{(0)}$ in the presence of the oscillating radio-frequency field. One can solve for the steady state with the field using a continued-fraction method, which gives a full series of elements $\rho_{11}^{(0)}(k)$, one for each Fourier component k. The inhomogeneous term on the right-hand side of Eq. (38) then becomes nonzero for all values of k instead of for one single component only. The equation can, however, be solved with the continued-fraction Green's function method.[25] The numerical work rapidly becomes rather involved, and we have chosen not to employ this method here. In the high-temperature limit, used here, the relaxation processes may be assumed fast enough to retain the totally in-

coherent distribution (47). We have chosen to look at the internal magnetic field splitting and the quadrupole splitting separately. Our method of approach does, however, allows us to include both without any additional computational complications. The ensuing spectra only become more complex. To facilitate interpretation we have chosen the numerical parameters such that the important physical features emerge in a transparent way. Especially our example ^{57}Fe derives its splitting from the internal field. In cases with small intrinsic splittings the Mössbauer components coalesce, and the interpretation of the spectrum becomes obscure. Also, less propitious parameter choices make the line shapes very complicated and the basic features mix into an unanalyzable multitude of features.

We have treated the case of a Mössbauer absorber. For the case of an emitter the treatment is analogous. The roles of the lower and upper levels are only interchanged, and the initially nonvanishing population is found in the distribution ρ_{22} instead of in ρ_{11} as assumed here. The algebraic treatment remains unaffected.

In conclusion, we have presented a density-matrix formulation of the theory of Mössbauer spectra. The γ-ray intensity is treated in lowest-order perturbation theory; we evaluate the linear response of the γ rays, and other perturbing effects are included in an exact way. The cases which reach steady state can be solved, and for a periodic external modulation the solution emerges as a matrix-continued fraction. This technique is applied to the case of magnetic modulation of Mössbauer spectra. The case of ^{57}Fe is treated as an example. Our solution includes saturation and interference effects due to large modulation amplitudes, and their effects on the spectra is evaluated and discussed.

ACKNOWLEDGMENTS

The authors gratefully acknowledge the continuing interest and support we have had from Professor T. Katila, Dr. E. Ikonen, and Dr. P. Helistö. They have introduced us to the phenomena, aided our progress during the research, and carefully scrutinized the present paper. Their suggestions and comments have been most helpful at every stage of our work.

*Present address: Department of Physics, University of California at Los Angeles, 405 Hilgard Ave., Los Angeles, CA 90024-1547.

[1]G. J. Perlow, Phys. Rev. **172**, 319 (1968).
[2]N. D. Heiman, L. Pfeiffer, and J. C. Walker, Phys. Rev. Lett. **21**, 93 (1968).
[3]G. Asti, G. Albanese, and C. Bucci, Phys. Rev. **184**, 260 (1969).
[4]L. Pfeiffer, J. Appl. Phys. **42**, 1725 (1971).
[5]L. Pfeiffer, N. D. Heiman, and J. C. Walker, Phys. Rev. B **6**, 74 (1972).
[6]C. L. Chien and J. C. Walker, Phys. Rev. B **13**, 1876 (1976).
[7]M. Kopcewicz, Phys. Status Solidi A **46**, 675 (1978).
[8]U. Olari, I. Popescu, and C. B. Collins, Phys. Rev. C **23**, 50 (1981).
[9]P. J. West and E. Matthias, Z. Phys. A **288**, 369 (1978).
[10]E. Ikonen, P. Helistö, J. Hietaniemi, and T. Katila, Phys. Rev. Lett. **60**, 643 (1988).
[11]M. N. Hack and M. Hammermesh, Nuovo Cimento **19**, 546 (1961).
[12]H. Gabriel, Phys. Rev. **184**, 359 (1969).
[13]A. V. Mitin, Phys. Lett. **84A**, 278 (1981).
[14]S. H. Autler and C. H. Townes, Phys. Rev. **100**, 703 (1955).
[15]S. Stenholm and W. E. Lamb, Jr., Phys. Rev. **181**, 618 (1969).
[16]S. Stenholm, J. Phys. B **5**, 878 (1972).
[17]S. Stenholm, J. Phys. B **5**, 890 (1972).
[18]M. Allegrini, E. Arimondo, and A. Bambini, Phys. Rev. A **15**, 718 (1977).
[19]A. Valli and S. Stenholm, Phys. Lett. **64A**, 447 (1978).
[20]H. Risken, *The Fokker-Planck Equation* (Springer-Verlag, Heidelberg, 1984).
[21]U. Fano, Phys. Rev. **131**, 259 (1963).
[22]A. J. Dekker, in *Hyperfine Interactions,* edited by A. J. Freeman and R. B. Frankel (Academic, New York, 1967), p. 679.
[23]M. Blume, Phys. Rev. **174**, 351 (1968); M. Blume and J. A. Tjon, *ibid.* **165**, 446 (1968); **165**, 456 (1968); M. J. Clauser and M. Blume, Phys. Rev. B **3**, 583 (1971).
[24]S. Stenholm, in *Essays in Theoretical Physics, In Honour of Dirk ter Haar,* edited by W. E. Parry (Pergamon, Oxford, 1984).
[25]C.-G. Aminoff and S. Stenholm, J. Phys. B **9**, 1039 (1976).